Appl. Phys. B 51, 171–176 (1990)

Applied Physics B Photophysics and Laser Chemistry



# Two-Wavelength Operation of a Femtosecond Ring Dye Laser

**N. I. Michailov, I. P. Christov, and I. V. Tomov**

Faculty of Physics, Sofia University, BG-1126 Sofia, Bulgaria

Received 8 September 1989/Accepted 15 November 1989

**Abstract.** We report on two-wavelength operation of a CPM ring dye laser employing Rhodamine 6G as gain medium and a new styryl dye as saturable absorber. Two trains of femtosecond pulses at different wavelengths are simultaneously generated under proper alignment of the laser. The secondary pulse train is attributed to the laser action of the absorber dye. Auto- and cross-correlation measurements are performed to determine the temporal characteristics of the laser in the double mode-locking regime.

**PACS:** 42.60

The mode-locked dye laser has become an important source of femtosecond optical pulses. The introduction of systems to control the intracavity group velocity dispersion (GVD) has led to routine generation of pulses shorter than 100 fs from both the purely passively mode-locked and hybrid synchronously pumped cw dye lasers. Rapid progress has been made during the last years in extending the wavelength coverage of such systems by using various novel active/passive dye combinations, see e.g. [Ref. 1, Table 3]. Recently we reported successful application of two new styryl dyes as saturable absorbers for mode-locking of cw Rhodamine 6G (Rh6G) dye laser in the spectral range 620–640 nm [2, 3]. These dyes, denoted in abbreviated form as TCVEB-iodide and TCETI-tetrafluoroborate, exhibit remarkable stability in contrast to the currently preferred mode-locker 3,3-diethyloxadicarbocyanine iodide (DODCI). When the dye 2-[2-(2,3,6,7-tetrahydro-1H, 5H-benzo[*i, j*]chinolizin-9-yl) ethenyl]-1,3,3-trimethyl-3H-indolinium tetrafluoroborate (TCETI tetrafluoroborate) was employed as saturable absorber, it was possible to adjust our colliding pulse mode-locked (CPM) ring dye laser in a characteristic mode of operation with two trains of short pulses at different wavelengths simultaneously generated [3]. Here we present results of the investigation of the double-pulsing operation of this laser.

## 1. Two-Wavelength Operation in CPM Ring Laser Configuration

The seven-mirror four-prism laser configuration is described elsewhere [3] and only a brief description will be given here. The mirrors used around the gain and absorber jets have radii of curvatures of 6.2 cm and 3.4 cm, respectively. The absorber jet thickness at the focal spot was approximately 50 μm. All the high reflectors have single stack $\lambda/4$ multilayer coatings centered at about 630 nm. The transmittance of the output coupling mirror varies from 1.2 to 1.4% in the spectral range 625–660 nm. The pulse durations were measured by standard autocorrelation technique using a 0.5 mm KDP frequency-doubling crystal and spectral information was acquired with a B & M optical multichanel analyzer (OSA 500).

We start from an optimized CPM laser yielding pulses shorter than 50 fs [3] around 640 nm in the usual mode of operation. Slight realignment of the end mirrors causes a sudden broadening of the autocorrelation trace in one of the directions of propagation in the ring. A distinct second spectral peak appears in this direction around 653 nm for values of the intracavity GVD in a narrow range, corresponding to the vicinity of the shortest pulses and for absorber jet positions close to the beam focus. Angle tuning of the frequency-doubling crystal in a collinear autocorrelation measurement reshapes the broaden autocorrelation in a triple-peaked trace shown in Fig. 1, which turns into

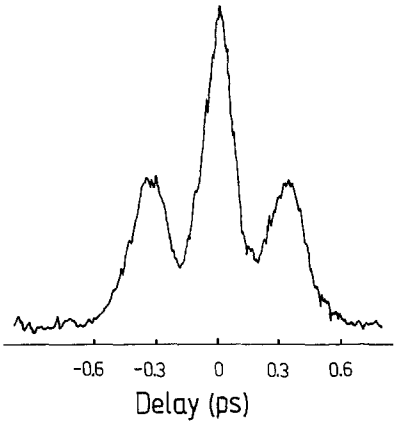


**Fig. 1.** Triple-peaked correlation trace obtained by angle tuning of the nonlinear crystal

two separate peaks with further angle tuning. At the same time the properties of the output beam in the other direction remain unaffected. This behavior was observed for TCETI concentrations above $\sim 1.5 \times 10^{-3}$ M. Autocorrelation data similar to those presented in Fig. 1 have been reported by others [4–6] for Rh 6G/DODCI-CPM lasers, as well as for other dye combinations [5, 7]. These observations have been attributed to the formation of higher-order solitons or soliton-like pulses where the triple-peaked autocorrelation represents a time average over the soliton period. However, we did not observe the characteristic periodic modulation that accompanied the higher-order soliton formation. No modulation was observed in the row and the filtered laser output, nor in the pulse power spectrum when a monochromator was tuned to a certain spectral components of the two parts of the laser spectrum. Therefore we concluded that two steady-state pulses at different wavelengths exist simultaneously, one of them being delayed with respect to the other, which yields the cross-correlation satellites superimposed on the autocorrelation peak in Fig. 1.

Simultaneous production of two pulses at different wavelengths, one of which is a higher-order soliton have been observed by Wise et al. [8]. The production of the second pulse train has been related to a soliton-reshaping mechanism similar to that creating a dispersive wave and a soliton in fibers around the zero-dispersion wavelength of the fiber. The evidence of a long-wavelength peak in the spectrum observed by Nighan et al. [6] is attributed to stimulated Raman scattering in the DODCI absorber, leading to an effect analogous to soliton self-frequency shift in fibers. We consider that the long-wavelength portion of the spectrum of our laser is due to the laser action of the TCETI dye, being intracavity synchronously pumped. We believe this interpretation is supported by the experimental results described below.

## 2. Role of the Cavity Dispersion for Efficient Double Mode-Locking

Double mode-locking (DML) with dye lasers has been realized most frequently with Rh 6G as gain medium and Cresyl Violet as saturable absorber. Two trains of picosecond pulses at different wavelengths have been generated with this dye combination in linear cavity configurations [9–11], as well as in a CPM ring laser [12]. Double pulsing with other dye pairs has also been demonstrated [13]. Compared to the standard synchronously pumped laser, the stringent requirements for cavity length matching and stabilizing are not necessary in the case of intracavity pumping. The dispersion of the cavity components, however, which defines the optical lengths of the two resonators, is of great importance for achieving optimum synchronous pumping, especially in the case of subpicosecond pulses. This could explain the fact that the long-wavelength spectral peak of our laser was observed in a very narrow range for intracavity GVD, close to the exact compensation point of the prism sequence.

The second spectral peak was very weak although the cross-correlation satellites in Fig. 1 were well resolved by appropriate angle tuning of the nonlinear crystal. In addition, the operation of the laser at near minimum pulse width is always accompanied by increased fluctuations, and the laser becomes highly sensitive to alignment and external perturbations. Therefore we have been unable to examine the basic features of the double-pulsing mode of operation with the laser configuration described above.

The best operation of the current laser in the spectral range up to 640 nm, where the absorption of TCETI is low, has been attributed to the existence of a photoisomer [3] as in the case of DODCI. We supposed that the main pulse wavelength falls in the long-wavelength side of the absorption curve of a transient absorbing species of TCETI which also lases, yielding the secondary pulse. It is interesting to note that laser action of DODCI, assigned to its photoisomer has been reported under extracavity excitation [14] and in a double mode-locked He–Ne laser too. [15]. With the above conjecture, more efficient pumping of the TCETI dye could be expected if the primary pulse wavelength is tuned toward the yellow. A CPM dispersion-controlled femtosecond laser at high absorber concentration is somewhat wavelength tunable only by varying the intracavity GVD. It was impossible, however, to obtain sufficient yellow shift and at the same time to keep the round-trip group delay times of the two pulses equal by increasing the negative GVD of the prism sequence alone. Two stable trains of short pulses at different wavelengths were clearly observed after replacement of one of the cavity mirrors by a

broadband double-stack mirror (with the blue stack on top). With this modification, it was possible to obtain adequate yellow shift of the primary pulse wavelength with generation of a sufficiently powerful second pulse train, which allowed pulse characteristics to be measured by alternate filtering of each spectral region of the DML laser output.

For an absorber jet position close to the beam waist and proper adjustment of the prism sequence dispersion, the laser enters the double-pulsing mode of operation after critical alignment of the cavity. The best DML was again unidirectional. The pulse properties in the single mode-locked (SML) direction remain unaffected, while the primary pulse in the DML direction broadens. Double mode-locking now exists in a comparatively wide region of the prism sequence GVD, which corresponds to a change of the intracavity glass path by about 3 mm. The wavelengths of the primary and the secondary pulse are simultaneously tuned in this region. Fig. 2 shows the variations of the two wavelengths as a function of the translated prism position. The variations of the autocorrelation widths for the three sets of pulses are also shown in the same figure. We shall indicate these three pulse trains as follows: (1) and (2) – primary and secondary pulse in the DML direction; (3) – pulse in the SML direction. We note here that under double mode-locking conditions only slight subsidence in the short-wavelength tail of the primary pulse spectrum appears in comparison to the laser spectrum in the SML direction.

The data presented in Fig. 2 were obtained in a concrete experimental situation. Double mode-locking was observed in wider spectral regions – 627–634 nm for the primary pulse, corresponding to a tuning of the secondary pulse wavelength from 658 nm to 647 nm. The typical laser outputs for the central part of the DML region shown in Fig. 2 are: ~4 mW in the SML direction; ~2.5 mW for the primary pulse train and ~1 mW for the secondary pulse train. The corresponding pump power of an argon ion laser was about 2.2 W.

The role of the broadband double-stack coated mirror for the efficiency of the DML, as well as the wavelength tuning capability can be explained by the dispersive properties of the mirror. The phase shift introduced by this mirror suffers significant variations with the wavelength within the high-reflectivity zone, see e.g. [16]. Figure 3 shows the calculated wavelength dependence of the mirror phase shift and its derivatives with respect to the frequency in the spectral range of interest [17]. The tuning ranges for the primary and secondary pulses are shown hatched in the figure. It can be seen that considerable negative GVD ($\phi'' > 0$) is introduced by this mirror in the spectral range 625–645 nm across the bandwidth of the primary

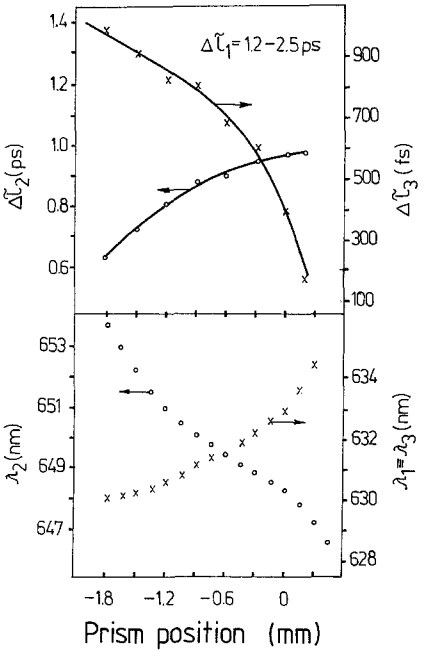


**Fig. 2.** Laser wavelength $\lambda_i$ and autocorrelation FWHM $\Delta\tau_i$ as a function of prism position for the three sets of pulses ($i=1$ – primary pulse in DML direction; $i=2$ – secondary pulse in DML direction; $i=3$ – pulse in SML direction). The higher values of prism positions correspond to more quartz in the cavity

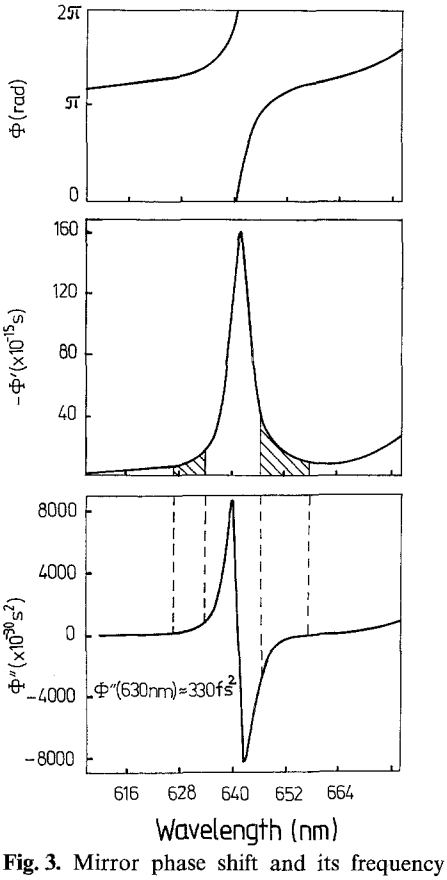


**Fig. 3.** Mirror phase shift and its frequency derivatives as a function of wavelength

pulse. At the same time, equal delay times are provided for two pulses whose wavelengths lie on the opposite slopes of the group delay curve (first derivative) around the minimum delay wavelength ~642 nm. Thus the mirror alone assures that the requirements for efficient intracavity synchronous pumping are met. The dispersion of the prism sequence also has to be added to the mirror dispersion, if we neglect the dispersive contribution of the other cavity components [18]. It should be noted that the zero position of the translated prism, depicted in Fig. 2, corresponds to a nearly symmetric arrangement of the two wavelengths around the zero dispersion wavelength of the prism sequence. Referring to the reported group delay spectra [Ref. 19, Fig. 2], it appears that the dispersion of the prism sequence, added to the mirror dispersion, equalizes the delay times in the hatched spectral ranges and reduces the curvature of the group delay curve. This facilitates the observed wavelength tuning capability.

The validity of the above considerations on the determinant role of the broadband mirror for efficient synchronous pumping was further confirmed by the fact that stable double-pulsing operation was also achieved with the prism sequence removed from the cavity.[1] The wavelengths of the primary and the secondary pulses in this case correspond to the zero prism position in Fig. 2. Another experimental observation deserves mention. It supports the assumption that the origin of the secondary pulse generation is the gain provided by the absorber dye, but not a soliton reshaping mechanism due to the combined action of the intracavity dispersion and self-phase modulation [8]. In the case where the prism sequence is removed from the cavity, we have been able to change the direction of double-pulsing operation by simple reversal of the absorber jet position relative to the beam focus. The relation between the disposition of the jet (left position or right position) and the corresponding direction of DML (clockwise or counter-clockwise) is consistent with the requirements for optimum pumping conditions with Gaussian beams [20]. For a jet position exactly at the focus, double pulsing becomes bidirectional. In this case the laser was very much less stable because of the competition between the two secondary pulses meeting in the mode-locking dye. In addition, double-pulsing operation was always accompanied by increased fluctuations, contrary to the observations which indicate soliton formation [8].

The variations of the characteristics of the three sets of pulses shown in Fig. 2 could be analyzed in terms of the cavity dispersion discussed above. The wavelength variation of the pulses produced by the Rh 6G gain ($\lambda_1 = \lambda_3$ curve) and the change of the pulse duration in the SML direction ($\Delta\tau_3$ curve) are typical for excess negative GVD. The shape of the $\Delta\tau_2$ curve is also explicable if the positive GVD in the corresponding spectral range is taken into account (Fig. 3). The behavior of the secondary pulse wavelength is not completely understood. The observed tuning does perhaps correspond generally to a self-adjusting of the secondary wavelength along the group delay curve, following the variation of the primary pulse group delay with wavelength. It follows from the behavior of the tuning curves presented in Fig. 2, that the creation of the secondary pulse cannot be related to a Raman shift in the absorber [6] ($\lambda_1$ and $\lambda_2$ shift in opposite directions). The tuning range of the secondary pulse wavelength is evidently restricted by the spectral region of positive gain within the fluorescence band of the TCETI dye and by the requirements for equality of the group delay times of primary and secondary pulses. The dramatic broadening of the primary pulse duration (ranging from 1.2 ps to 2.5 ps from left to right in Fig. 2) is not now clear. The DML mechanism is not fully clarified so far. The theoretically predicted shortening of the primary pulse [21] has been not clearly demonstrated in the experiment. The transition from a long-pulse (ns) operation of a mode-locked dye laser to the picosecond range [9], which had been attributed to the lasing of the absorber, is most likely related to the adjustment of the laser parameters [12] (e.g. raising the absorber concentration and wavelength tuning). We note that a primary pulse broadening similar to that observed, has been reported for a double mode-locked He–Ne laser [15].

## 3. Temporal Properties of the Mode-Locked Trains

Correlation measurements were performed to determine the temporal characteristics of the laser in the DML regime. A set of autocorrelation traces corresponding to a prism position around the zero point of the DML range (Fig. 2) is shown in Fig. 4a. It was found [3] that for excess negative GVD the pulse in the usual mode-locked direction is well fitted with an asymmetric exponential-like intensity profile of the type

$$I(t) = \{\exp[t/\tau(1+a)] + \exp[-t/\tau(1-a)]\}^{-2}. \quad (1)$$

Several pulse shapes were used to fit the experimental autocorrelations of the secondary pulse. The best fit was obtained for symmetric double-sided exponential intensity profile, although the shape (1) also yields quite similar theoretical autocorrelation for values of the asymmetry parameter $a$ between 0.75 and 0.5. We

[1] In the case of a cavity arrangement with all single stack mirrors the laser is well into the unstable regime [3] without the prism sequence

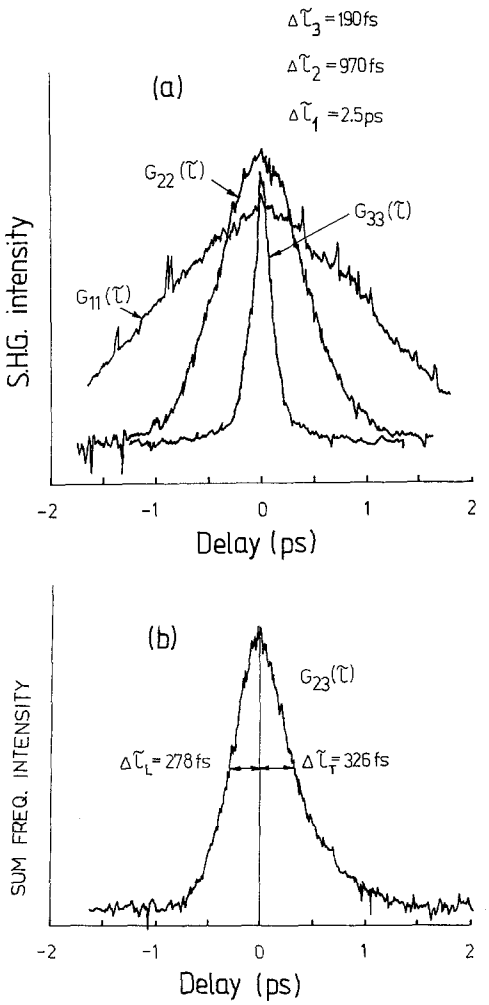


**Fig. 4. a** A set of experimental autocorrelations of the three pulse trains; **b** Measured cross-correlation between secondary pulse and pulse in the SML direction; $\Delta\tau_L$ and $\Delta\tau_L$ are widths of the leading and the trailing edge of the cross-correlation

tried to glean more information regarding pulse shape with the help of cross-correlation measurements. For a range of prism positions (right-hand side of Fig. 2) the pulse in the SML direction is very narrow in comparison with the others. Therefore the former could be used as a sampling (impulse) function to display approximately the shape of the longer pulses. The cross-correlation measurements were performed by collinear sum-frequency generation in the same nonlinear crystal used in the autocorrelation measurements. The cross-correlation between the secondary pulse and the pulse in the SML direction was measured by the aid of an extracavity variable delay. Fig. 4b presents the cross-correlation $G_{23}(\tau)$ between the pulses whose autocorrelations are shown in Fig. 4a. If we assume an asymmetric pulse shape of the type (1) for both pulses, the FWHM $\Delta t_3$ of the pulse in the SML direction exceeds 120 fs and the secondary pulse width

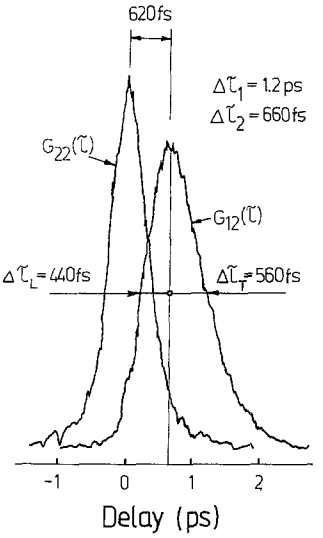


**Fig. 5.** Cross-correlation between primary and secondary pulses together with autocorrelation of the secondary pulse, both measured with a red filter inserted in the fixed arm of the autocorrelator. Cross-correlation FWHM is 1 ps

$\Delta t_2$ is greater than 620 fs [Ref. 22, Table 1]. It follows from the value of the measured cross-correlation width ($\Delta\tau_L + \Delta\tau_T = 604$ fs), that the symmetric double-sided exponential shape which yields $\Delta t_2 = 400$ fs is a much better fit to the secondary pulse. The slight asymmetry of the measured cross-correlation can be attributed to an asymmetric jitter [10], which also causes some broadening of the cross-correlation. By similar auto- and cross-correlation measurements it was found that the primary pulse is also highly symmetric in shape and a symmetric double-sided exponential intensity profile could be used as a good approximation.

The synchronism and the time delay between the two pulses in the DML direction were also investigated by cross-correlation measurements. Figure 5 shows a cross-correlation $G_{12}(\tau)$ together with the autocorrelation $G_{22}(\tau)$ of the secondary pulse, both measured with a red filter inserted in the fixed arm of the autocorrelator. A yellow filter in the variable arm is unnecessary because the phase matching acts as a filter (the spectral separation of the two wavelengths was about 25 nm in this case). The FWHM of the theoretical cross-correlation, corresponding to the pulse durations depicted in Fig. 5, is 910 fs if we assume a symmetric double-sided exponential shape for both the primary and the secondary pulse. It could be calculated from the results presented in Fig. 5 that the jitter figure of merit [10] is 90 fs. A low random jitter between the two pulse trains is typical for the DML operation. A glance at the results presented in Fig. 4b shows that, as expected, in a CPM laser, the jitter between the secondary pulse train and the pulse train in the SML direction is also very low. According to the

estimations given in [10], it follows from the value of the interpulse jitter that the magnitude of a possible shift of the cross-correlation trace toward longer $\tau$ (caused by an asymmetric jitter) is far below the measured delay of 620 fs between the two curves shown in Fig. 5. Evidently in this case the secondary pulse occurs prior to the arrival of the primary pulse peak. Similar relative time positions of the two pulses produced by a double mode-locked dye laser have been observed by others [10] in the case of an incompletely mode-locked secondary pulse. We have at present no explanation of this temporal correlation between the pulses. It could be calculated and it was experimentally confirmed that this temporal relation of the two pulses was not caused by the dispersion of a certain part of the laser cavity and that it remains nearly the same through the whole laser cavity. It seems, in contrast to the theoretical predictions, that the secondary pulse grows at the leading edge of the pumping (primary) pulse, which also significantly broadens under DML conditions.

The autocorrelation shown in Fig. 5 is the shortest recorded and implies a secondary pulse duration of 270 fs, assuming a symmetric double-sided exponential shape. The corresponding spectral bandwidth was 1.2 nm, yielding a time-bandwidth product of 0.23 (transform-limited value of 0.14).

## 4. Conclusion

We have demonstrated double mode-locking in the femtosecond range with a CPM ring dye laser, employing Rh 6G as gain medium and the styryl dye TCETI as saturable absorber. Two highly synchronous fs pulse trains at different wavelengths are generated simultaneously by proper alignment and optimization of the laser. The important role of the dispersion of a broadband double-stack coated mirror for achieving efficient intracavity pumping is revealed. The measured pulse durations, the degree of synchronism and the cross-correlation widths are, to the authors knowledge, the best so far reported for a double mode-locked dye laser. A symmetric double-sided exponential pulse shape was found to be a good approximation for both the primary and the secondary pulse. The secondary pulse grows at the leading edge of the pumping pulse, which, in addition, significantly broadens. Because of this broadening, the unidirectional DML operation of this laser (which yields two femtosecond pulse trains at different wavelengths) is an obvious advantage of the ring configuration for application purposes.

## References


1. A. Penzkofer: Appl. Phys. B **46**, 43–60 (1988)
2. N. Michailov, T. Deligeorgiev, V. Petrov, I. Tomov: Opt. Commun. **70**, 137–140 (1989)
3. N.I. Michailov, T.G. Deligeorgiev, I.P. Christov, I.V. Tomov: Opt. Quantum Electron. (to be published)
4. F. Salin, P. Grangier, G. Roger, A. Brun: Phys. Rev. Lett. **56**, 1132–1135 (1986); Phys. Rev. Lett. **60**, 569–572 (1988)
5. H. Avramopoulos, P.M.W. French, J.A.R. Williams, G.H.C. New, J.R. Taylor: IEEE J. QE-**24**, 1884–1892 (1988)
6. W.L. Nighan, Jr., T. Gong, P.M. Fauchet: Opt. Lett. **14**, 447–449 (1989)
7. P. Georges, F. Salin, G. Le Saux, G. Roger, A. Brun: Opt. Commun. **69**, 281–286 (1989)
8. F.W. Wise, I.A. Walmsley, C.L. Tang: Opt. Lett. **13**, 129–131 (1988)
9. Z.A. Yasa, A. Dienes, J.R. Whinnery: Appl. Phys. Lett. **30**, 24–26 (1977)
10. E. Bourkoff, A. Dienes: IEEE J. QE-**16**, 425–433 (1980)
11. G. Arjavalingham, A. Dienes, J.R. Whinnery: Opt. Lett. **5**, 193–195 (1982)
12. K.K. Li, G. Arjavalingam, A. Dienes, J.R. Whinnery: IEEE J. QE-**19**, 539–543 (1983)
13. N.J. Frigo, H. Mahr, D.J. Erskine: IEEE J. QE-**18**, 192–198 (1982)
14. M. Maeda: *Laser Dyes* (Academic Tokyo, 1984) pp. 33–34, and references therein
15. P.K. Runge: Opt. Commun. **5**, 311–313 (1972)
16. P. Laporta, V. Magni: Appl. Opt. **24**, 2014–2020 (1985)
17. These calculations based on the matrix formulation for multilayer filters were performed by A.S. Grytzkov and the results were kindly presented to us
18. S. De Sivestry, P. Laporta, O. Svelto: IEEE J. QE-**20**, 533–539 (1984)
19. W.H. Knox, N.M. Pearson, K.D. Li, C.A. Hirlimann: Opt. Lett. **13**, 574–576 (1988)
20. B.B. Snavely: In *Dye Lasers*, ed. by F.P. Schäfer, Topics Appl. Phys. **1** (Springer, Berlin, Heidelberg 1973) p. 99
21. Z.A. Yasa: J. Appl. Phys. **46**, 4895–4898 (1975)
22. J.C. Diels, J.J. Fontain, I.C. Mc Michael, F. Simoni: Appl. Opt. **24**, 1270–1282 (1985)


*Responsible for Advertisements:* E. Lückermann, G. Probst, Heidelberger Platz 3, D-1000 Berlin 33, Tel. (030) 8207-0, Telex 01-85411, FAX (0) 30/8207300
*Responsible for the Text:* H. K. V. Lotsch, Tiergartenstrasse 17, D-6900 Heidelberg, Tel. (0) 6221/487253, Telex 461723, FAX (0) 6221/43982
Printers: Brühlsche Universitätsdruckerei, Giessen

Springer-Verlag GmbH & Co. KG, D-1000 Berlin 33